Journal of Microbiology (2019) Vol. 57, No. 4, pp. 252–262
DOI 10.1007/s12275-019-8531-y
eISSN 1976-3794
pISSN 1225-8873

Co-occurrence patterns between phytoplankton and bacterioplankton across the pelagic zone of Lake Baikal during spring[§]

Ivan S. Mikhailov[1,2*], Yuri S. Bukin[1,2], Yulia R. Zakharova[1,2], Marina V. Usoltseva[1], Yuri P. Galachyants[1,2], Maria V. Sakirko[1], Vadim V. Blinov[1], and Yelena V. Likhoshway[1,2]

[1]*Limnological Institute, Siberian Branch of the Russian Academy of Sciences, Irkutsk, Russia*
[2]*Irkutsk Scientific Center, Siberian Branch of the Russian Academy of Sciences, Irkutsk, Russia*

(Received Sep 27, 2018 / Revised Nov 9, 2018 / Accepted Nov 26, 2018)

Phytoplankton and bacterioplankton play a key role in carbon cycling of aquatic ecosystems. In this study, we found that co-occurrence patterns between different types of phytoplankton, bacterioplankton, and environmental parameters in Lake Baikal during spring were different over the course of three consecutive years. The composition of phytoplankton and bacterial communities was investigated using microscopy and 16S rRNA gene pyrosequencing, respectively. Non-metric multidimensional scaling (NMDS) revealed a relationship between the structure of phytoplankton and bacterial communities and temperature, location, and sampling year. Associations of bacteria with diatoms, green microalgae, chrysophyte, and cryptophyte were identified using microscopy. Cluster analysis revealed similar correlation patterns between phytoplankton abundance, number of attached bacteria, ratio of bacteria per phytoplankton cell and environmental parameters. Positive and negative correlations between different species of phytoplankton, heterotrophic bacteria and environmental parameters may indicate mutualistic or competitive relationships between microorganisms and their preferences to the environment.

Keywords: co-occurrence patterns, phytoplankton, bacterioplankton, algal-bacterial associations, Lake Baikal

Introduction

Phytoplankton and bacterioplankton are the foundation of the microbial food web and play an important role in biogeochemical cycles of aquatic ecosystems (Azam and Malfatti, 2007; Fuhrman, 2009). During spring blooms, phytoplankton produces organic matter that is consumed by specific groups of heterotrophic bacteria. This trophic chain leads to synchronization of planktonic bacteria growth with phytoplankton bloom (Teeling *et al*., 2012; Buchan *et al*., 2014; Tan *et al*., 2015). Types of interactions between microalgae and bacteria vary from mutualism to antagonism and competition for biogenic elements (Amin *et al*., 2012). Many bacteria associate with phytoplankton (Grossart *et al*., 2005; Sison-Mangus *et al*., 2014) and are attached to healthy or dying cells (Mayali *et al*., 2011; Smriga *et al*., 2016), as they feed on the released dissolved organic matter, breaking down the dead algal cell (Bidle and Azam, 1999) or generating algicidal compounds (Mayali and Azam, 2004). Phytoplankton blooms in close associations with bacteria as imposed by their dependence on vitamins, recycled nutrients, assimilable iron or amino acids (Amin *et al*., 2012).

In aquatic ecosystems, the structure of microbial communities changes in space and time along with such parameters as depth, salinity, temperature, pH, hydrological conditions, nutrients, organic matter, and interspecies interactions (Fortunato *et al*., 2013). Seasonal patterns of bacterial communities and specific bacterial groups can be strongly repeatable and depend on daylight hours, temperature, nutrients, and photosynthetically-active radiation (Gilbert *et al*., 2012). Co-occurrence patterns revealed on the basis of biotic and abiotic parameters can be used to predict ecological interactions between various species and environmental parameters in aquatic ecosystems (Eiler *et al*., 2012; Paver *et al*., 2013; Pearman *et al*., 2015; Bunse *et al*., 2016).

Lake Baikal is the world's largest freshwater lake in terms of volume (Shimaraev *et al*., 1994). In the spring, after the ice cover is gone (May through June), a massive phytoplankton bloom dominated by diatoms (13–98% of phytoplankton biomass) takes place in the lake. The composition of phytoplankton species in the pelagic zone of the lake is prone to interannual variability (Popovskaya *et al*., 2015). Bacterial communities in different basins of the lake with different dominant types of phytoplankton have a similar composition (Mikhailov *et al*., 2015). Earlier, we used 454 pyrosequencing of 16S rRNA and 18S rRNA genes to study bacterial and eukaryotic microbial communities, and their co-occurrence patterns in Lake Baikal during spring. We found that microbes within one domain mostly were correlated positively with each other and were highly interconnected (Mikhailov *et al*., 2019).

The aims of this study were (1) to reveal the relationships between phytoplankton, bacterial communities, and environmental factors, and (2) to investigate algal-bacterial associations in Lake Baikal during spring in different years. Over the course of three years, we analyzed phytoplankton and heterotrophic bacteria using microscopy and culturing, respec-

*For correspondence. E-mail: ivanmikhai@gmail.com; Tel.: +7-3952-42-65-04; Fax: +7-3952-42-54-05
[§]Supplemental material for this article may be found at http://www.springerlink.com/content/120956.

tively. Total bacterial abundance, algal-bacteria associations and the structure of bacterial communities were analyzed in the course of two years, using epifluorescence, scanning electron microscopy, and pyrosequencing. Co-occurrence patterns were identified based on quantitative data for phytoplankton and bacteria and physicochemical parameters at 30 stations in the pelagic zone of the lake during spring (2011–2013).

Materials and Methods

Study area and sampling

The samples for 2011 and 2013 were collected using the same methods as for 2012 (Mikhailov *et al.*, 2019) at 30 stations in Lake Baikal (Fig. 1) from depths of 0 to 25 m from 27 May to 6 June 2011; from 3 June to 11 June 2012; and from 20 May to 7 June 2013.

Physicochemical analyses

The following abiotic parameters were measured: temperature (T), dissolved oxygen (O_2), phosphate concentration (PO_4^{3-}), nitrates (NO_3^-), silicon (Si), and acidity (pH). The measurements were carried out as previously described (Mikhailov *et al.*, 2019).

Estimation of phytoplankton and bacterioplankton

Analysis of phytoplankton and bacterioplankton was performed for integrated water samples (200 ml samples collected from the 0, 5, 10, 15, 20, and 25 m layers, with a total volume of 1.2 L).

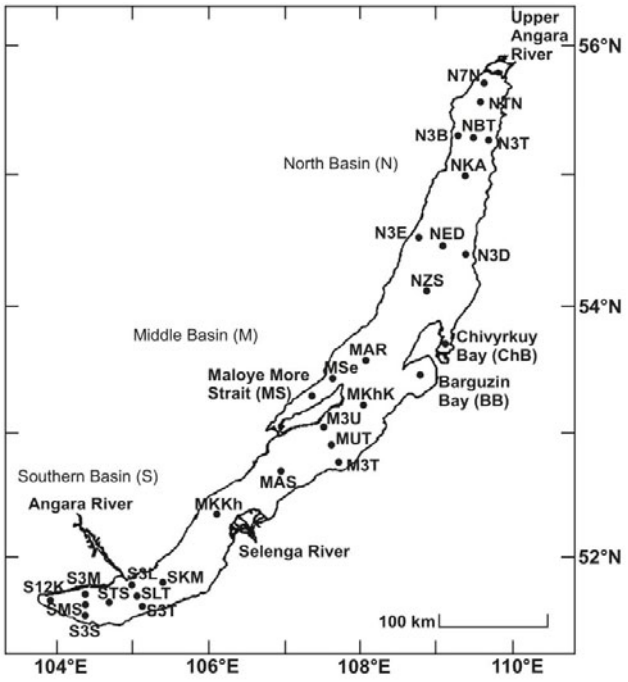

Fig. 1. Map of sampling stations at Lake Baikal.

For quantification and identification of phytoplankton by light microscopy, 1.2 L of every integrated sample, fixed with Lugol's solution, was concentrated by settling and siphoning. Phytoplankton was counted, and its biomass and composition were evaluated using the method described in previous work (Popovskaya *et al.*, 2015). Data on total biomass and phytoplankton composition in 2011 and 2012 were obtained earlier (Mikhailov *et al.*, 2015; Popovskaya *et al.*, 2015).

Water samples preserved in glutaraldehyde (Sigma-Aldrich) were stained with 4,6-diamidino-2-phenylindole (DAPI, Sigma, final concentration 1 μg/ml) for 15 min (Porter and Feig, 1980) and filtered through a polycarbonate membrane (0.2 μm) (Millipore) using Sartorius filter units. Bacterial cells were enumerated using an Axiovert 200 inverted microscope (Carl Zeiss). For total bacterial abundance, counts were taken of at least 20 fields of view per sample. Phytoplankton-attached bacteria were counted for 1,000 fields of view across the entire filter area. The vast majority of attached bacteria was clearly focused on through several optical planes and counted in planes clearly different from surface of the 0.2 μm pore-size filter where the free-living bacteria were. Careful focusing at different planes allows for counting of the attached bacteria on both sides of phytoplankton, as the cells are semi-transparent in the DAPI-stained preparations (Znachor *et al.*, 2012). Microphotographs were taken with a PIXERA Penguin 600CL camera with the AxioSet program.

To calculate the number of heterotrophic bacteria, 1 ml water samples from the 0, 5, 10, 15, 20, and 25 m layers were inoculated in 10% fish peptone agar (FPA) and diatom agar (DA) as described earlier (Zakharova *et al.*, 2010). Colony-forming units (CFU) were measured after a 7-day incubation period at 20°C.

Analyses of diatom-bacterial assemblages using scanning electron microscope (SEM)

Forty microliters of a phytoplankton mesh sample fixed with 1% glutaraldehyde solution was placed on a 0.2 μm polycarbonate filter and air dried. The sample was dewatered in ethanol solutions of 30%, 50%, 70%, and 96%, and then dried. A filter holding the sample was then fixed at a SEM screen and coated with gold in a vacuum unit SDC 004 (Balzers). Samples were examined under the scanning electron microscopes Philips 525M and FEI Quanta 200.

DNA extraction, PCR amplification, and 454 pyrosequencing

Previously, we have analyzed water samples collected in 2012 using pyrosequencing V3-V4 regions of 16S rRNA genes (Mikhailov *et al.*, 2015, 2019). Four water samples were collected in 2013 and DNA was extracted from them as described earlier (Mikhailov *et al.*, 2019). The V3-V4 region of the 16S rRNA gene was amplified by PCR using the universal primers U341F (5′-CCTACGGGRSGCAGCAG-3′) and U785R (5′-GGACTACCVGGGTATCTAAKCC-3′) (Baker *et al.*, 2003). Sequencing of the 2013 samples was carried out on a GS 454 FLX genome sequencer (Roche) using Titanium reagents in Limnological Institute SB RAS. The sequences were deposited in the NCBI Short Read Archive (SRA) under the accession numbers PRJNA275679 for 2012 and PRJNA484671 for 2013.

Pyrosequencing data from 2012 and 2013 were combined into one array which was analyzed using Mothur 1.19.0 software (Schloss *et al.*, 2009). The data were processed using the PyroNoise algorithm (Quince *et al.*, 2011). The sequences were grouped into operational taxonomic units of the species level (OTUs) with 97% similarity. For genetic distance calculations, only substitutions in the nucleotide were used. The obtained sequences were classified by the Ribosomal Database Project (RDP) with bootstrap support of at least 80%. The diversity estimators (OTU numbers, Shannon index, Simpson index) were calculated for each sample based on the OTUs identified using package "vegan" (Oksanen *et al.*, 2016) in R.

Statistical analysis

A bootstrap coefficient (Smith and van Belle, 1984) and rarefaction curve were calculated to evaluate statistical representativeness of 16S rRNA reads. For multivariate statistical analyses and hypothesis testing, abundance counts of bacterial OTUs were normalized to the relative abundance of reads per sample. Clustering of communities was performed using the Bray-Curtis dissimilarity matrix and UniFrac metric with UPGMA. Ordination was performed by NMDS (Bray-Curtis dissimilarity matrix and UniFrac metric) and constrained correspondence analysis (CCA). We used correlation analysis and Spearman's *r* correlation coefficient (Hollander and Wolfe, 1973) to identify pairwise associations between (a) biomass of phytoplankton, abundance of bacterioplankton and environmental parameters, as well as (b) abundance of certain species of phytoplankton and its attached bacteria, ratio of bacteria per phytoplankton cell and environmental parameters. The accuracy of the correlation coefficients was determined using 'W' Spearman statistics (Royston, 1995), for which the null hypothesis was rejected if its probability was lower than the critical level where $\alpha = 0.05$. The *P* values were corrected for the false discovery rate in multiple comparisons using the Benjamini-Hochberg equation (Benjamini and Hochberg, 1995). Also, the correlation matrix was visualized through a network using "igraph" packages in R (Csardi and Nepusz, 2006). The network topology is based on the number of links and correlation coefficients between neighboring nodes. The more links the nodes form among themselves, the closer they are placed in the network.

Distribution of the ratio of bacteria per phytoplankton cell was visualized in violin plots using the "vioplot" package in R. Correlation coefficients calculated for algal-bacterial associations and environmental parameters were aggregated into a matrix that was visualized by a heat map generated using "gplots" (Warnes *et al.*, 2009) in R. With the help of the "gplots" package, lines and columns in the correlation matrix were clustered and grouped in order of similarity (Euclidean distance metric and the complete-link clustering method).

The uncertainty of hierarchical clustering in this work was assessed by multiscale bootstrap resampling in the "pvclust" package (Suzuki and Shimodaira, 2006) with 1,000 bootstrap replicates.

Regression analysis was used to evaluate correlations between environmental parameters and abundance of a certain species of phytoplankton and its attached bacteria, and the ratio of bacteria per phytoplankton cell. Linear and exponential dependences were tested as regression models. The best model was selected based on a covariation coefficient (R^2) and Akaike information criterion (AIC) (Akaike, 1998). Regression analysis was done using the least-square method in R.

Results

Abiotic environmental parameters and phytoplankton composition

In 2012, the ice cover removal at Lake Baikal occurred earlier than in 2011 and 2013 (Supplementary data Fig. S1). The average water temperature was the highest in 2012 (2.52–4.57°C) and the lowest in 2013 (1.31–3.41°C) (Supplementary data Fig. S2). From 2011 to 2013, the pH in the 0 to 25 m layer varied between 7.66 and 8.4; oxygen concentration (O_2) was in the range of 11.75–13.63 mg/L, silicon (Si) was 0.43–0.98 mg/L, phosphates (PO_4^{3-}) were 0.013–0.031 mg/L and nitrates (NO_3^-) were 0.22–0.37 mg/L (Supplementary data Table S1).

Cluster analysis showed that most phytoplankton communities from 2011, 2012, and 2013 were clustered together on the dendrogram, while some 2011 communities of northern basin were clustered separately (Supplementary data Fig. S3). Communities from 2011 and 2013 were grouped together within a large cluster (Supplementary data Fig. S3). In 2011, the total biomass of phytoplankton (TBP) in the lake varied from 2.4 mg/m^3 to 0.45 g/m^3 (Popovskaya *et al.*, 2015) (Supplementary data Table S2). Diatom *Synedra acus* subsp. *radians* (Kütz.) Skabitsch. [= *Fragilaria radians* (Kütz.) D.M.Williams & Round] dominated in the southern and middle basins, while *Gymnodinium baicalense* Antipova dominated in the northern basin of the lake (Popovskaya *et al.*, 2015) (Supplementary data Table S2). In 2012, the TBP in the pelagic zone (from 66 mg/m^3 to 1 g/m^3) was lower than in the bays and the strait (Mikhailov *et al.*, 2015) (Supplementary data Table S2). *S. acus* subsp. *radians* dominated in the southern basin, while *Aulacoseira baicalensis* (K. Meyer) Simonsen diatom dominated in the northern basin. Dinoflagellates *G. baicalense* and *Peridinium baicalense* Kiselev and Zvetkov were dominant at several stations of the middle basin (Mikhailov *et al.*, 2015) (Supplementary data Table S2). In 2013, the TBP varied from 35 mg/m^3 to 0.86 g/m^3 (Supplementary data Table S2). *G. baicalense*, *Aulacoseira islandica* (O. Müller) Simonsen, and *A. baicalensis* dominated in the southern basin in terms of biomass, while *S. acus* subsp. *radians* dominated in the middle basin and *Nitzschia gracilliformis* Lange-Bertalot & Simonsen was dominant at several stations of the northern basin (Supplementary data Table S2).

Distribution and composition of bacterioplankton

In 2011 and 2012, total bacterial abundance (TBA) varied between 0.2×10^6 cells/ml to 1.5×10^6 cells/ml in the surface layer (0 m) and the upper 0 to 25 m layer (Supplementary data Fig. S4). Abundance of heterotrophic bacteria in the DA medium tended to be lower than in the FPA medium (Supplementary data Fig. S5). In 2011, the largest number of heterotrophs was found in the surface layer of the southern and middle basins, reaching 482 CFU/ml (Supplementary

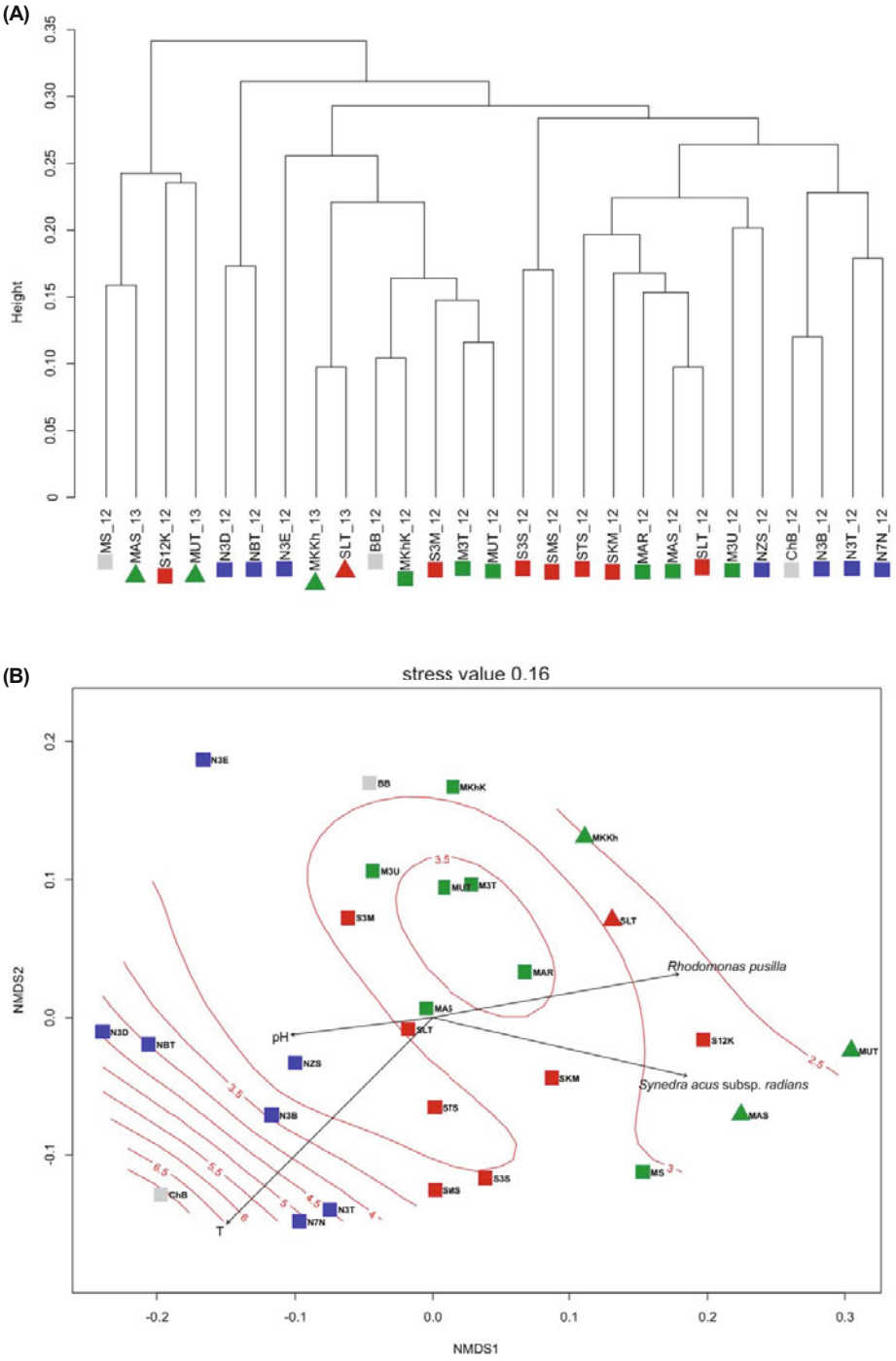

Fig. 2. Cluster analysis completed for OTUs (97%) of bacterial communities of 2012 and 2013 with UniFrac metric (A). NMDS biplot completed for bacterial communities with UniFrac metric (B). Squares and triangles show samples of 2012 and 2013, respectively. Red, green, and blue figures show stations of the south, middle, and north Baikal basins, respectively. Gray designates stations of the bays and strait. The fitted vectors show abiotic and biotic variables. Red lines show temperature gradient.

data Fig. S5A and B). In 2012, the largest number of heterotrophs was found at 5 to 20 m depths in the middle and northern basins (Supplementary data Fig. S5C and D). In the DA medium, the number of heterotrophs reached 585 CFU/ml in the middle basin and 2,320 CFU/ml in the northern basin and the strait (Supplementary data Fig. S5C). In the FPA medium, the number of heterotrophs was 1,250 CFU/ml in the middle basin and 2,800 CFU/ml in the northern basin (Supplementary data Fig. S5D). In 2013, the largest number of heterotrophs was detected in the northern basin at the 25 m depth, reaching 1,200 CFU/ml (Supplementary data Fig. S5E and F). The number of CFUs at the 0, 5, 10, 15, 20, and 25 m layers were positively correlated with each other in all years (Supplementary data Table S3). Correlations among bacteria in different water layers are probably related to water mixing in the lake during spring (Shimaraev *et al.*, 1994).

The analysis, using rarefaction curve (Supplementary data Fig. S6) and bootstrap index (Supplementary data Table S4), showed adequate coverage for samples from 2012 and 2013 with an exception of MKKh12, NED12, and NTN12 which

Table 1. The effects of environmental factors on composition of phytoplankton and bacterial evaluated with unconstrained ordination with NMDS and CCA analysis
Bold denotes accurate values.

Controlling factors in bacterial communities				
Parameter	NMDS R2	NMDS *P*_value	CCA F	CCA *P*_value
pH	0.086	0.357	**2.160**	**0.037**
T	**0.355**	**0.001**	1.347	0.262
Synedra acus* subsp. *radians	**0.288**	**0.018**	0.731	0.698
Rhodomonas pusilla	**0.264**	**0.014**	**2.606**	**0.021**
basin	**0.485**	**0.001**	**2.848**	**0.009**
Year of sampling	**0.243**	**0.001**	**5.497**	**0.000**
Controlling factors in phytoplankton communities				
Parameter	NMDS R2	NMDS *P*_value	CCA F	CCA *P*_value
O_2	**0.209**	**0.001**	0.830	0.750
Si	**0.255**	**0.001**	2.127	0.190
T	**0.349**	**0.001**	1.580	0.280
CFU on FPA	**0.211**	**0.001**	0.896	0.630
TBP	**0.262**	**0.001**	2.199	0.125
basin	0.101	0.122	**7.488**	**0.005**
Year of sampling	**0.456**	**0.001**	**6.734**	**0.005**

had a high share of undetected OTUs in the top 90% of the data pool and were therefore deleted. Bacterial communities in the southern and middle basins in 2012 and 2013 had a similar number of OTUs, Shannon index and Simpson index (Supplementary data Table S4). Bacterial communities included members of *Actinobacteria*, *Bacteroidetes*, *Verrucomicrobia*, *Proteobacteria*, *Acidobacteria*, *Cyanobacteria*, *Planctomycetes*, TM7 and bacteria unclassified phyla (Supplementary data Fig. S7). The communities of 2012 had a higher Bacteroidetes ratio (9–25%) than communities of 2013 (3–7.5%) (Supplementary data Fig. S7). Community clustering using the UniFrac metric revealed that bacterial communities in the southern and middle basins in 2012 and 2013 were clustered together in the dendrogram (Fig. 2A), which indicates their similarity with each other.

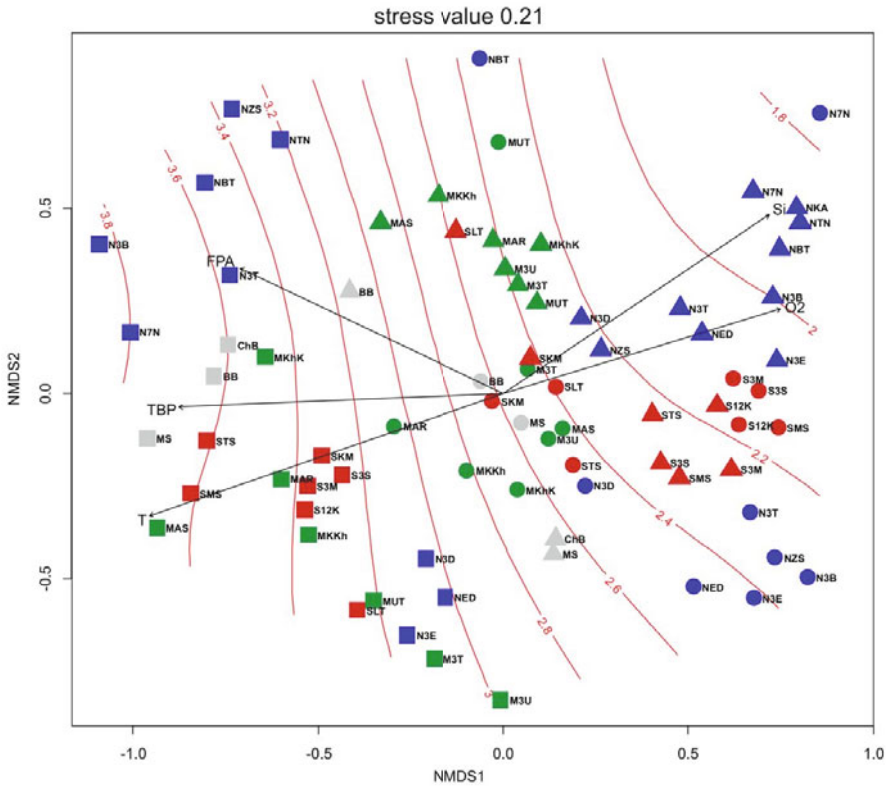

Fig. 3. NMDS biplot completed for phytoplankton communities of 2011–2013 with Bray Curtis dissimilarity index. The fitted vectors show physicochemical variables. Circles, squares, and triangles show samples of 2011, 2012, and 2013, respectively. Red, green, and blue figures show stations of the south, middle, and north Baikal basins, respectively. Gray designates stations of the bays and strait. Red lines show temperature gradient.

Relationship among bacterioplankton, phytoplankton, and environmental parameters

The structure of bacterial communities was related to temperature and biomasses of *S. acus* subsp. *radians* and *Rhodomonas pusilla* (H.Bachmann) Javornicky (Fig. 2B and Table 1). CCA revealed a relationship between a sampling location (i.e. a particular basin), sampling year, pH, *R. pusilla* biomass, and community composition (Table 1). The structure of phytoplankton communities was related to temperature, TBP, Si, CFU on FPA, O_2, sampling year and location (Table 1). CCA found a relationship between a sampling year, location, and community composition. Phytoplankton communities in 2012 had the largest biomass and developed at the highest temperatures and CFU counts on FPA and the lowest levels of Si and O_2, compared to other years (Fig. 3). The direction of vectors on the NMDS plot shows that Si and O_2 were positively correlated with each other and negatively correlated with temperature, TBP, and CFU on FPA (Fig. 3). Analysis of temperature isolines shows that temperatures were different in three years; therefore, the effect of the year can be related to the temperature differences. Communities located in close proximity to each other were clustered together, which could be due to their similar composition and environment.

We performed a correlation analysis for the biomass of certain phytoplankton species and relative abundance of 16S rRNA reads (27 samples from 2012 and 4 samples from 2013). The meaningfulness of bacterial OTU clustering was verified using the bootstrap method. A group of bacterial OTUs belonging to *Betaproteobacteria* (OTU008 and OTU-0018 *Rhodoferax*, OTU0032 Methylophilaceae), *Planctomycetes* (OTU0047 and OTU0049 Phycisphaeraceae), *Actinobacteria* (OTU004 and OTU005 Acidimicrobineae), and *Flavobacteria* (OTU0061 *Fluviicola*) formed an accurate cluster that was positively correlated with the biomass of *S. acus* subsp. *radians*, *Peridinium baicalense*, *Gymnodinium baicalense*, *Cyclotella baicalensis* Skvortzov and Meyer, and *Dinobryon cylindricum* O.E.Imhof (Supplementary data Fig. S8).

Correlation patterns between different species of phytoplankton, bacterioplankton, and abiotic parameters differed in the spring over the course of three years (Fig. 4). In 2011, diatoms (*S. acus* subsp. *radians*, *A. baicalensis*, *A. islandica*, *Stephanodiscus meyeri* Genkal and Popovskaya) were negatively correlated with Si. *S. acus* subsp. *radians* and had a negative correlation with NO_3^-, while *S. meyeri* was negatively correlated with PO_4^{3-} (Fig. 4A). In 2012, *S. acus* subsp. *radians* and *A. baicalensis* correlated negatively with Si and PO_4^{3-}, respectively (Fig. 4B). In 2013, *A. baicalensis* and *A. islandica* had a negative correlation with Si, while *N. graciliformis* had a positive one. *Monoraphidium griffithii* (Berkeley) Komárková-Legnerová was correlated positively with NO_3^- (Fig. 4C).

Biomasses of centric diatoms *A. baicalensis*, *A. islandica*, and *S. meyeri* were positively correlated with each other in 2011 and 2013 (Fig. 4A and C). Pennate diatom *S. acus* subsp.

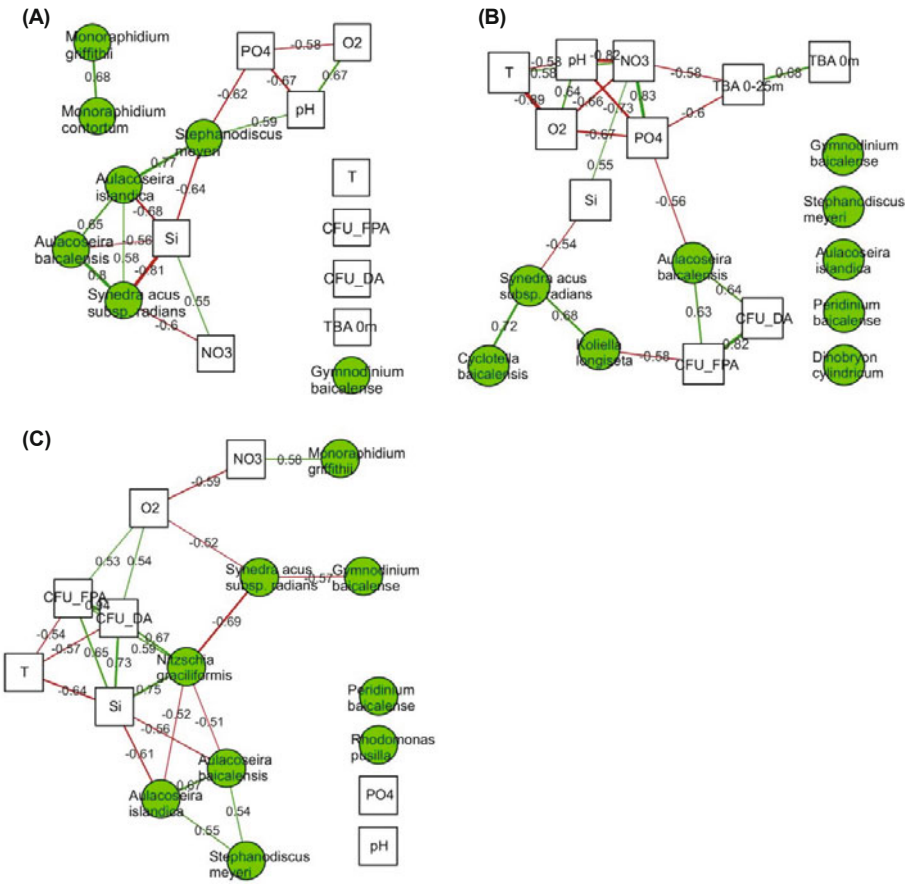

Fig. 4. Correlation networks of biomass of different species of phytoplankton, abundance of bacterioplankton and abiotic environmental factors in the photic layer of Lake Baikal in spring 2011 (A), 2012 (B), 2013 (C). The network shows significant correlations ($\alpha = 0.05$) for 2011 $r \geq |0.55|$; for 2012 $r \geq |0.54|$; for 2013 $r \geq |0.5|$. Green lines show positive correlations; red lines show negative correlations. Green circles are species of phytoplankton; white squares – biotic and abiotic parameters. Correlation coefficients are displayed on the lines. The length and width of the connecting lines are equivalent to correlation values.

radians had a positive correlation with centric diatoms (*Aulacoseira*, *Stephanodiscus*) in 2011 (Fig. 4A), and centric diatom *C. baicalensis* and green microalgae *Koliella longiseta* (Vischer) Hindák in 2012 (Fig. 4B). In 2013, *S. acus* subsp. *radians* was negatively correlated with small-celled pennate *N. graciliformis* and dinoflagellate *G. baicalense* (Fig. 4C). Green microalgae *M. griffithii* and *Monoraphidium contortum* (Thuret) Komárková-Legnerová had positive correlations with each other (Fig. 4A), while *N. graciliformis* was negatively correlated with other diatoms (Fig. 4C). Heterotrophic bacteria (CFU) were positively correlated with *A. baicalensis* and negatively correlated with *K. longiseta* in 2012 (Fig. 4B). CFU were positively correlated with *N. graciliformis* in 2013 (Fig. 4C).

Analysis of algal-bacterial assemblages

Scanning electron microscopy revealed that bacteria in the shape of rods, flagella, cocci, diplococci, and filamentous bacteria colonized cell walls of different diatoms in Lake Baikal (Fig. 5). Bacteria were located on the surface of cells of *Aulacoseira baicalensis* (Fig. 5F) and *Synedra acus* subsp. *radians* (Fig. 5A and D) or formed assemblages at junctions of diatom cells (Fig. 5E and G). In some cases, bacteria formed biofilms combining several cells of diatoms *S. acus* subsp. *radians* into aggregates (Fig. 5C).

Quantitative characteristics of algal-bacterial associations in the photic layer in 2011 and 2012 samples were evaluated using epifluorescent microscopy. Bacterial associations with diatoms (Supplementary data Fig. S9A–G), green microalgae (Supplementary data Fig. S9H–J), chrysophyte (Supplementary data Fig. S9K), and cryptophyte (Supplementary data Fig. S9L) were detected. Bacteria were found on some cells of dinoflagellates. The ratio of bacteria per phytoplankton cell in the surface layer (0 m) was the similar for all stations, being 1.86 ± 0.18 in 2011 and 2.42 ± 0.22 in 2012. Further, statistical analysis for the 0 m layer was done for the combined two years. Ratio of bacteria per phytoplankton cell in the surface layer varied from 0.95 ± 0.5 to 5.09 ± 0.72 across all stations (Supplementary data Fig. S10A), and from 0.13 ± 0.13 to 5.03 ± 2.55 in the upper 0 to 25 m layer in 2012 (Supplementary data Fig. S10B). Each station had different ratios of bacteria per phytoplankton cell in the 0 m and 0 to 25 m layers (Supplementary data Fig. S10).

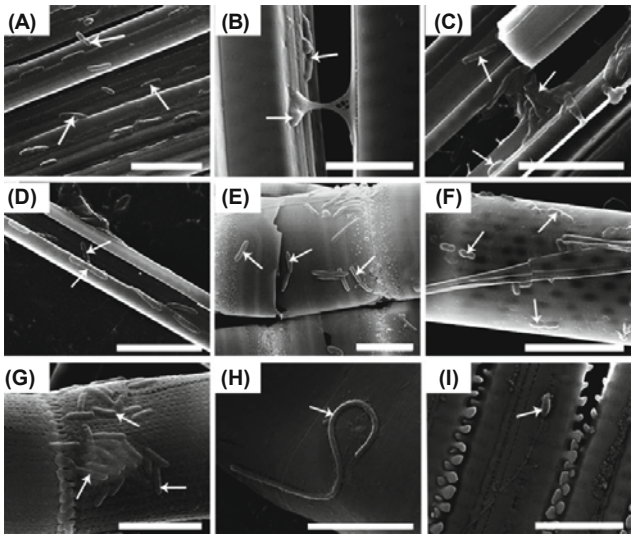

Fig. 5. Algal-bacterial associations of plankton in Lake Baikal in spring. (A, B, C, D) *S. acus* subsp. *radians*; (E) *St. meyeri*; (F, H) *A. baicalensis*; (G) *A. islandica*; (I) *F. crotonensis*. Arrows show bacteria. Scanning electron microscopy. Scale: (A, C–E, G, H) 5 μm; (B, I) 3 μm; (F) 10 μm.

The ratio of bacteria per phytoplankton cell in the 0 m layer was the highest for *S. acus* subsp. *radians* (4.54 ± 0.33), *N. gracilifomis* (3.9 ± 0.51), and *D. cylindricum* (3.22 ± 0.7), compared to other species. The following pairs had a similar ratio of bacteria per phytoplankton cell: *A. baicalensis* and *A. islandica*; *G. baicalense* and *R. pussila*; *M. contortum* and *M. griffithii* (Supplementary data Fig. S11A). The ratio of bacteria per phytoplankton cell in the 0–25 m layer in 2012 was higher for *S. acus* subsp. *radians* (4.57 ± 0.78), *D. cylindricum* (4.51 ± 0.6), and *N. gracilifomis* (3.7 ± 0.67), compared to other phytoplankton species (Supplementary data Fig. S11B). It follows that the ratio of bacteria per cell of different species of phytoplankton in the 0 m and 0 to 25 m layers was similar in two years (Supplementary data Fig. S11).

The number of attached bacteria was positively correlated with the number of phytoplankton host species (Supplementary data Table S4). Significant correlation coefficients varied between 0.72 (*R. pusilla*) and 0.97 (*S. acus* subsp. *radians*) for the 0 m layer, and 0.74 (*A. islandica*) and 0.97 (*N. graciliformis*, *D. cylindricum*) for the 0 to 25 m layer (Supplementary data Table S5).

Heatmap clustering shows that the number of phytoplankton and its attached bacteria and the ratio of bacteria per phytoplankton cell have similar correlation patterns with environmental parameters in water layer 0 m (Fig. 6A) and 0 to 25 m (Fig. 6B). In the 0 m layer (Fig. 6A), one cluster of correlations of algal-bacterial associations with PO_4^{3-}, NO_3^-, Si and TBA, and a second correlation cluster with FPA and DA (heterotrophic bacteria), O_2 and pH were identified. In the 0 to 25 m layer (Fig. 6B), one cluster of correlations of algal-bacterial associations with PO_4^{3-}, NO_3^-, Si, FPA, and DA and another correlation cluster with biomass of phytoplankton species, TBA, O_2, and pH were revealed.

Generally, correlation between the number of phytoplankton species identified by epifluorescent microscopy and environmental parameters was similar to outcomes of the correlation analysis of biomass of phytoplankton species and environmental parameters. This is evidenced by a positive correlation between abundance of phytoplankton biomass identified by a settling method and phytoplankton abundance identified by counting on filters (Fig. 6B).

Discussion

This work shows that correlations between phytoplankton, bacterioplankton, and abiotic parameters of Lake Baikal in the spring were different during three consecutive years (Fig. 4). Such factors as sampling location (i.e. the lake's basin), sampling year and temperature influenced the structure of bacterial (Fig. 2B) and phytoplankton (Fig. 3) communities. This could be due to differences in timing for ice cover removal (Supplementary data Fig. S1) and water temperature

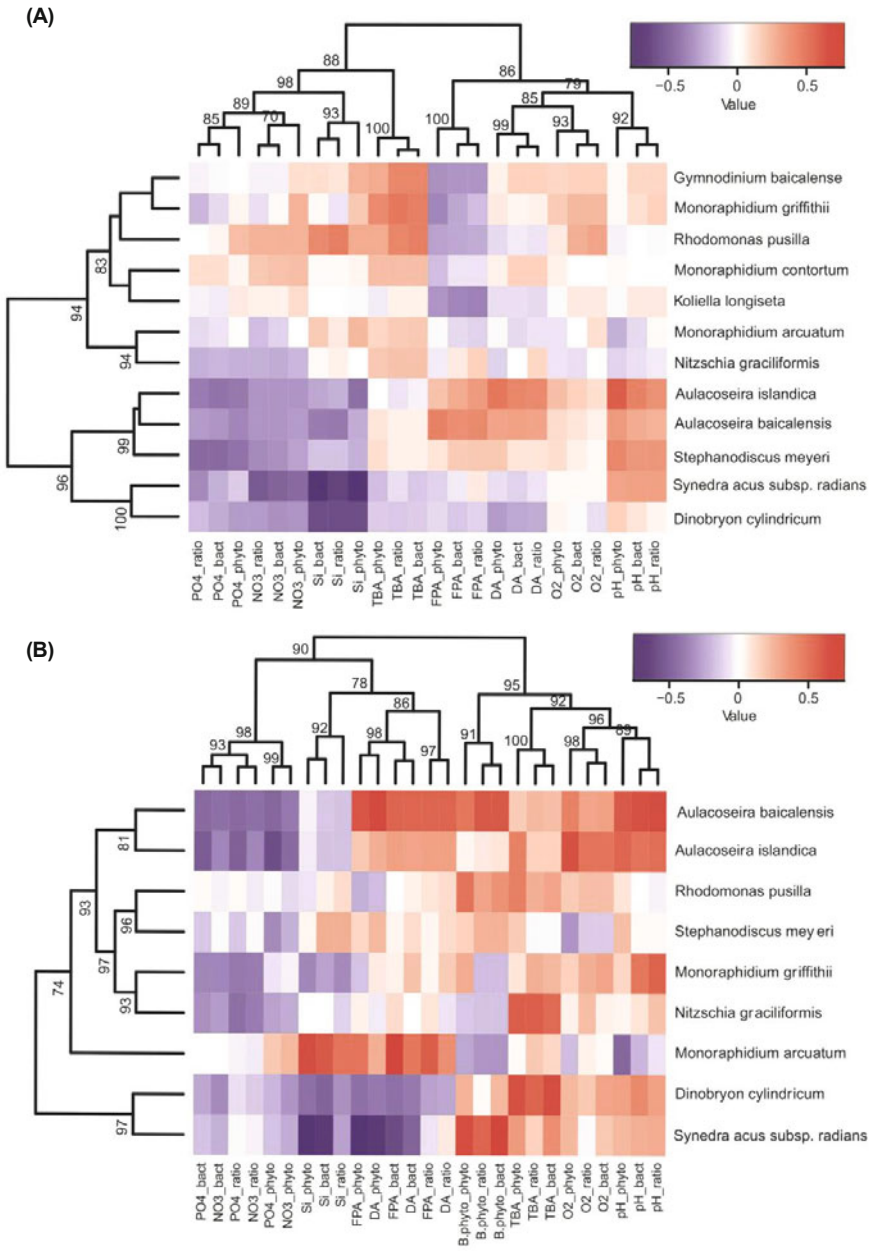

Fig. 6. A heatmap showing correlations among environmental parameters with abundance of different species of phytoplankton, abundance of attached bacteria, and ratio of bacteria per phytoplankton cell in Lake Baikal for 0 m (A), and 0–25 m (B). On the right are the species of phytoplankton for which correlations were determined. Below are the pairs of environmental parameters and parts of algal-bacterial associations that were examined for correlation. bact, abundance of attached bacteria; phyto, abundance of phytoplankton species; ratio, ratio of bacteria per phytoplankton cell. B. phyto, biomass of appropriate phytoplankton species determined by the settling method. Colors indicate the r values of Spearman's rank correlation coefficients. Bootstrap supports in percent are shown on the dendrogram.

(Supplementary data Fig. S2) in three years. Weather conditions at the lake and distribution of biogenic elements and phytoplankton in the pelagic zone could also be different in different years (Domysheva *et al.*, 2014; Khodzher *et al.*, 2017).

Conducting a correlation analysis for biomass of individual phytoplankton species rather than for the total phytoplankton biomass allowed us to more thoroughly identify correlations between phytoplankton and nutrients. We found significant correlations between the biomass of individual phytoplankton species and nutrients such as Si, NO_3^-, and PO_4^{3-} (Fig. 4). Earlier studies showed that correlations between total phytoplankton biomass and concentrations of NO_3^-, PO_4^{3-} and temperature were weak, while those with Si concentration varied widely (Pomazkina *et al.*, 2010; Popovskaya *et al.*, 2015).

Correlation relationships between phytoplankton species were different in three years (Fig. 4). Centric diatoms *A. baicalensis*, *A. islandica*, and *S. meyeri* had positive correlations between each other in 2011 and 2013 (Fig. 4A and C). Pennate diatom *S. acus* subsp. *radians* was correlated with different phytoplankton species in different years (Fig. 4). Heterotrophic bacteria were positively correlated with *A. baicalensis* (Fig. 4B) and *N. graciliformis* (Fig. 4C). Positive correlations may indicate a mutualistic relationship, while negative correlations may indicate a competitive one. Differences in the environment in three years influence the phytoplankton composition, and potentially interspecies interactions. Co-occurrence network analysis is used to predict direct associations between taxa, and can be used to deter-

mine the general preference of taxa for specific environmental factors (Eiler *et al.*, 2012; Faust and Raes, 2012; Vacher *et al.*, 2016). Microbes also may positively or negatively correlate for indirect reasons, based on their environmental preferences (Weiss *et al.*, 2016).

We showed that phytoplankton cells are colonized by bacteria (Supplementary data Figs. S9–S11) of different forms (Fig. 5) during spring in Lake Baikal. It is known that phytoplankton cells are surrounded by the phycosphere, containing extracellular metabolites consumed by heterotrophic bacteria (Amin *et al.*, 2012). Up to 40% of carbon dioxide fixed by photosynthesis in a diatom is used to produce extracellular polymeric substances (Fogg, 1983) that act as a source of nutrients for heterotrophic bacteria (Sarmento and Gasol, 2012). The number of attached bacteria was positively correlated with the number of phytoplankton host species (Supplementary data Table S5). The number of bacteria associated with phytoplankton is correlated with phytoplankton dynamics more closely than the number of free-living bacteria, which indicates the presence of specific interactions between phytoplankton and its attached bacteria (Rooney-Varga *et al.*, 2005). The number of bacteria increases during the final stages of phytoplankton bloom in freshwater (Rösel and Grossart, 2012) and marine ecosystems (Teeling *et al.*, 2012). Succession of bacterial groups that are adapted to consumption of certain organic matter is observed during phytoplankton bloom (Teeling *et al.*, 2012; Buchan *et al.*, 2014). Phytoplankton composition was different between two years (Supplementary data Table S2), while composition of bacterial communities was similar (Supplementary data Fig. S7). During spring phytoplankton blooms in the southern North Sea (German Bight), phytoplankton species (including diatoms) were different in the course of four consecutive years, although the composition of bacteria that increased in number during phytoplankton blooms was similar. The phytoplankton blooms trigger secondary blooms of bacterial communities that consist of swift successions of distinct bacterial clades, most prominently members of the *Flavobacteria*, *Gammaproteobacteria*, and the alphaproteobacterial *Roseobacter* clade (Teeling *et al.*, 2016). During early spring diatom bloom in Xiangshan Bay, *Rhodobacteraceae*, *Flavobacteriaceae*, and *Microbacteriaceae* were the main bacterial families in bacterial communities (Zhang *et al.*, 2018).

We found that bacterial biofilms combined several cells of diatoms such as *S. acus* subsp. *radians* into aggregates (Fig. 5C). Bacteria initiate formation of aggregates with diatom cells, causing aggregates to settle deeper down the water column (Gärdes *et al.*, 2011). Earlier, it was found that cells of *S. acus* subsp. *radians* in the top layer of the sediment in the southern basin were colonized by bacteria located on the surface and inside dead cells of diatoms, which accounted for up to 48% of total bacterial abundance (1.4×10^6 cells/ml) (Zakharova *et al.*, 2013). It follows that bacteria consume exometabolites of live diatoms and colonize their cell walls in the top water layers. They can also contribute to destruction of diatoms when those sink to the bottom. Bacteria use different enzymes to hydrolyze organic matter of live and dead diatoms which causes the dissolution of siliceous cell walls, representing an important stage in the carbon and silica cycles (Bidle and Azam, 1999, 2001).

We selected *S. acus* subsp. *radians* that dominated in the water samples and the Si concentration to analyze the type of relationship between algal-bacterial associations and environmental parameters. At the 0 and 0 to 25 m layers, the abundance of *S. acus* subsp. *radians* and its attached bacteria had a negative correlation with Si (r = -0.75, r = -0.66, respectively) (Fig. 6). An exponential regression model (the lowest AIC value) was used to describe the relationship between diatoms and their attached bacteria with Si (Fig. 7). An exponential increase in the number of diatoms (Fig. 7A) was followed by an exponential increase in the number of attached bacteria (Fig. 7B) and a reduction in silicon concentration (Fig. 7), as silicon accumulates to build up cell walls of diatoms. A reduction in silicon concentration is followed by an increase in the ratio of bacteria per phytoplankton cell (Fig. 7C). This happens when the number of attached bacteria increases at a rate higher than that of phytoplankton (Fig. 7).

In this work, we found that co-occurrence patterns among phytoplankton, bacterioplankton, and abiotic parameters

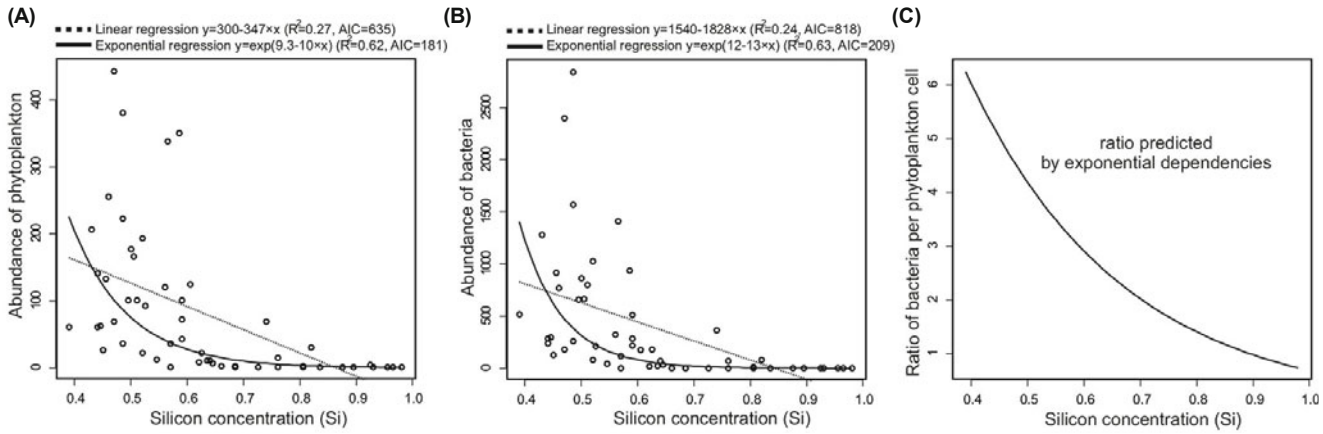

Fig. 7. Regression graphs showing the relationships between abundance of diatom *S. acus* subsp. *radians* and the silicon concentration (A), abundance of attached bacteria of *S. acus* subsp. *radians* and silicon concentration (B), and theoretically calculated ratio of bacteria per phytoplankton cell and silicon concentration (C). Equations of the linear and exponential regression model are provided.

across pelagic zone of Lake Baikal in spring were different in three years. The number of attached bacteria was positively correlated with different phytoplankton species. Space and time factors influenced the structure of phytoplankton and bacterial communities.

Acknowledgements

This work was supported by the ISC SB RAS integration project No. AAAA-A17-117041250054-8 "Basic research and innovative technologies as a basis for advanced development of Baikal region and its interregional relationships", project 4.2. "Application of the NGS-BD methods to ecological problems" (metagenomic and statistical analyses), FASO projects No. 0345-2016-0005 (sequencing), No. 0345-2016-0001 (microscopy), and No. 0345-2016-0008 (hydrochemical analyses). The study was performed using microscopes of the Instrument Center "Electron Microscopy" of the Shared Research Facilities for Physical and Chemical Ultramicroanalysis LIN SB RAS. We thank R. Yu. Gnatovsky from the Hydrology and Hydrophysics laboratory of LIN of SB RAS for collecting water samples; the Irkutsk Supercomputer Center of SBRAS for providing the access to HPC-cluster "Akademik V.M. Matrosov"; and Ivan Sidorov, system administrator of HPC-cluster, for help in performing computations.

References

Akaike, H. 1998. Information theory and an extension of the maximum likelihood principle, pp. 199–213. *In* Selected papers of Hirotugu Akaike, Springer, New York, NY, USA.

Amin, S.A., Parker, M.S., and Armbrust, E.V. 2012. Interactions between diatom and bacteria. *Microbiol. Mol. Biol. Rev.* **76**, 667–684.

Azam, F. and Malfatti, F. 2007. Microbial structuring of marine ecosystems. *Nat. Rev. Microbiol.* **5**, 782–791.

Baker, G.C., Smith, J.J., and Cowan, D.A. 2003. Review and re-analysis of domain-specific 16S primers. *J. Microbiol. Methods* **55**, 541–555.

Benjamini, Y. and Hochberg, Y. 1995. Controlling the false discovery rate: a practical and powerful approach to multiple testing. *J. R. Stat. Soc. Ser. B Methodol.* **57**, 289–300.

Bidle, K.D. and Azam, F. 1999. Accelerated dissolution of diatom silica by marine bacterial assemblages. *Nature* **397**, 508–512.

Bidle, K.D. and Azam, F. 2001. Bacterial control of silicon regeneration from diatom detritus: Significance of bacterial ectohydrolases and species identity. *Limnol. Oceanogr.* **46**, 1606–1623.

Buchan, A., Le Cleir, G.R., Gulvik, C.A., and González, J.M. 2014. Master recyclers: features and functions of bacteria associated with phytoplankton blooms. *Nat. Rev. Microbiol.* **12**, 686–698.

Bunse, C., Bertos-Fortis, M., Sassenhagen, I., Sildever, S., Sjöqvist, C., Godhe, A., Gross, S., Kremp, A., Lips, I., Lundholm, N., *et al.* 2016. Spatio-temporal interdependence of bacteria and phytoplankton during a Baltic Sea spring bloom. *Front. Microbiol.* **7**, 1–10.

Csardi, G. and Nepusz, T. 2006. The igraph software package for complex network research. *Int. J. Complex Syst.* **1695**, 1–9.

Domysheva, V.M., Usoltseva, M.V., Sakirko, M.V., Pestunov, D.A., Shimaraev, M.N., Popovskaya, G.I., and Panchenko, M.V. 2014. Spatial distribution of carbon dioxide fluxes, biogenic elements, and phytoplankton biomass in the pelagic zone of Lake Baikal in spring period of 2010–2012. *Atmos. Ocean. Opt.* **27**, 529–535.

Eiler, A., Heinrich, F., and Bertilsson, S. 2012. Coherent dynamics and association networks among lake bacterioplankton taxa. *ISME J.* **6**, 330–342.

Faust, K. and Raes, J. 2012. Microbial interactions: from networks to models. *Nat. Rev. Microbiol.* **10**, 538–550.

Fogg, G.E. 1983. The ecological significance of extracellular products of phytoplankton photosynthesis. *Bot. Mar.* **26**, 3–14.

Fortunato, C.S., Eiler, A., Herfort, L., Needoba, J.A., Peterson, T.D., and Crump, B.C. 2013. Determining indicator taxa across spatial and seasonal gradients in the Columbia River coastal margin. *ISME J.* **7**, 1899–1911.

Fuhrman, J.A. 2009. Microbial community structure and its functional implications. *Nature* **459**, 193–199.

Gärdes, A., Iversen, M.H., Grossart, H.P., Passow, U., and Ulrich, M.S. 2011. Diatom-associated bacteria are required for aggregation of *Thalassiosira weissflogii*. *ISME J.* **5**, 436–445.

Gilbert, J.A., Steele, J.A., Caporaso, J.G., Steinbrück, L., Reeder, J., Temperton, B., Huse, S., McHardy, A.C., Knight, R., Joint, I., *et al.* 2012. Defining seasonal marine microbial community dynamics. *ISME J.* **6**, 298–308.

Grossart, H.P., Levold, F., Allgaier, M., Simon, M., and Brinkhoff, T. 2005. Marine diatom species harbour distinct bacterial communities. *Environ. Microbiol.* **7**, 860–873.

Hollander, M. and Wolfe, D.A. 1973. Nonparametric statistical methods. John Wiley & Sons, New York, USA.

Khodzher, T.V., Domysheva, V.M., Sorokovikova, L.M., Sakirko, M.V., and Tomberg, I.V. 2017. Current chemical composition of Lake Baikal water. *Inland Waters* **7**, 250–258.

Mayali, X. and Azam, F. 2004. Algicidal bacteria in the sea and their impact on algal blooms. *J. Eukaryot. Microbiol.* **51**, 139–144.

Mayali, X., Franks, P.J.S., and Burton, R.S. 2011. Temporal attachment dynamics by distinct bacterial taxa during a dinoflagellate bloom. *Aquat. Microb. Ecol.* **63**, 111–122.

Mikhailov, I.S., Zakharova, Y.R., Bukin, Y.S., Galachyants, Y.P., Petrova, D.P., Sakirko, M.V., and Likhoshway, Y.V. 2019. Co-occurrence networks among bacteria and microbial eukaryotes of Lake Baikal during a spring phytoplankton bloom. *Microb. Ecol.* **77**, 96–109.

Mikhailov, I.S., Zakharova, Y.R., Galachyants, Y.P., Usoltseva, M.V., Petrova, D.P., Sakirko, M.V., Likhoshway, Y.V., and Grachev, M.A. 2015. Similarity of structure of taxonomic bacterial communities in the photic layer of Lake Baikal's three basins differing in spring phytoplankton composition and abundance. *Dokl. Biochem. Biophys.* **465**, 413–419.

Oksanen, J., Blanchet, F.G., Friendly, M., Kindt, R., Legendre, P., McGlinn, D., Minchin, P.R., O'Hara, R.B., Simpson, G.L., Solymos, P., *et al.* 2016. Vegan: Community ecology package. version 2.4-1. https://CRAN.R-project.org/package=vegan.

Paver, S.F., Hayek, K.R., Gano, K.A., Fagen, J.R., Brown, C.T., Davis-Richardson, A.G., Grabb, D.B., Rosario-Passapera, R., Giongo, A., Triplett, E.W., *et al.* 2013. Interactions between specific phytoplankton and bacteria affect lake bacterial community succession. *Environ. Microbiol.* **15**, 2489–2504.

Pearman, J.K., Casas, L., Merle, T., Michell, C., and Irigoien, X. 2015. Bacterial and protist community changes during a phytoplankton bloom. *Limnol. Oceanogr.* **61**, 198–213.

Pomazkina, G.V., Belykh, O.I., Domysheva, V.M., Sakirko, M.V., and Gnatovskii, R.Y. 2010. Structure and dynamics of the phytoplankton in Southern Baikal (Russia). *Int. J. Algae* **12**, 64–79.

Popovskaya, G.I., Usol'tseva, M.V., Domysheva, V.M., Sakirko, M.V., Blinov, V.V., and Khodzher, T.V. 2015. The spring phytoplankton in the pelagic zone of Lake Baikal during 2007–2011. *Geogr. Nat. Resour.* **36**, 253–262.

Porter, K.G. and Feig, Y.S. 1980. The use of DAPI for identifying and counting aquatic microflora. *Limnol. Oceanogr.* **25**, 943–948.

Quince, C., Lanzen, A., Davenport, R.J., and Turnbaugh, P.J. 2011. Removing noise from pyrosequenced amplicons. *BMC Bioinformatics* **12**, 1–18.

Rooney-Varga, J.N., Giewat, M.W., Savin, M.C., Sood, S., LeGresley, M., and Martin, J.L. 2005. Links between phytoplankton and bacterial community dynamics in a coastal marine environment. *Microb. Ecol.* **49**, 163–175.

Royston, P. 1995. Remark AS R94: a remark on algorithm AS 181: the W-test for normality. *J. R. Stat. Soc. Ser. C Appl. Stat.* **44**, 547–551.

Rösel, S. and Grossart, H.P. 2012. Contrasting dynamics in activity and community composition of free-living and particle-associated bacteria in spring. *Aquat. Microb. Ecol.* **66**, 169–181.

Sarmento, H. and Gasol, J.M. 2012. Use of phytoplankton-derived dissolved organic carbon by different types of bacterioplankton. *Environ. Microbiol.* **14**, 2348–2360.

Schloss, P.D., Westcott, S.L., Ryabin, T., Hall, J.R., Hartmann, M., Hollister, E.B., Lesniewski, R.A., Oakley, B.B., Parks, D.H., Robinson, C.J., *et al.* 2009. Introducing mothur: open-source, platform-independent, community-supported software for describing and comparing microbial communities. *Appl. Environ. Microbiol.* **75**, 7537–7541.

Shimaraev, M.N., Verbolov, V.I., Granin, N.G., and Sherstayankin, P.P. 1994. Physical limnology of Lake Baikal: a review. Baikal Int. Center for Ecological Research, Irkutsk Okayama, Japan.

Sison-Mangus, M.P., Jiang, S., Tran, K.N., and Kudela, R.M. 2014. Host-specific adaptation governs the interaction of the marine diatom, *Pseudo-nitzschia* and their microbiota. *ISME J.* **8**, 63–76.

Smith, E.P. and van Belle, G. 1984. Nonparametric estimation of species richness. *Biometrics* **40**, 119–129.

Smriga, S., Fernandez, V.I., Mitchell, J.G., and Stocker, R. 2016. Chemotaxis toward phytoplankton drives organic matter partitioning among marine bacteria. *Proc. Natl. Acad. Sci. USA* **113**, 1576–1581.

Suzuki, R. and Shimodaira, H. 2006. Pvclust: an R package for assessing the uncertainty in hierarchical clustering. *Bioinformatics* **22**, 1540–1542.

Tan, S., Zhou, J., Zhu, X., Yu, S., Zhan, W., Wang, B., and Cai, Z. 2015. An association network analysis among microeukaryotes and bacterioplankton reveals algal bloom dynamics. *J. Phycol.* **51**, 120–132.

Teeling, H., Fuchs, B.M., Becher, D., Klockow, C., Gardebrecht, A., Bennke, C.M., Kassabgy, M., Huang, S., Mann, A.J., Waldmann, J., *et al.* 2012. Substrate-controlled succession of marine bacterioplankton populations induced by a phytoplankton bloom. *Science* **336**, 608–611.

Teeling, H., Fuchs, B.M., Bennke, C.M., Krüger, K., Chafee, M., Kappelmann, L., Reintjes, G., Waldmann, J., Quast, C., Glöckner, F.O., *et al.* 2016. Recurring patterns in bacterioplankton dynamics during coastal spring algae blooms. *Elife* **5**, e11888.

Vacher, C., Tamaddoni-Nezhad, A., Kamenova, S., Peyrard, N., Moalic, Y., Sabbadin R., Schwaller, L., Chiquet, J., Smith, M.A., Vallance, J., *et al.* 2016. Chapter one-learning ecological networks from next-generation sequencing data. *Adv. Ecol. Res.* **54**, 1–39.

Warnes, G.R., Bolker, B., Bonebakker, L., Gentleman, R., Huber, W., Liaw, W.H.A., Lumley, T., Maechler, M., Magnusson, A., Moeller, S., *et al.* 2009. Gplots: Various R programming tools for plotting data. *R package version* 2.4.

Weiss, S., Van Treuren, W., Lozupone, C., Faust, K., Friedman, J., Deng, Y., Xia, L.C., Xu, Z.Z., Ursell, L., Alm, E.J., *et al.* 2016. Correlation detection strategies in microbial data sets vary widely in sensitivity and precision. *ISME J.* **10**, 1669–1681.

Zakharova, Y.R., Adel'shin, R.V., Parfenova, V.V., Bedoshvili, Y.D., and Likhoshway, Y.V. 2010. Taxonomic characterization of the microorganisms associated with the cultivable diatom *Synedra acus* from Lake Baikal. *Microbiology* **79**, 679–687.

Zakharova, Y.R., Galachyants, Y.P., Kurilkina, M.I., Likhoshvay, A.V., Petrova, D.P., Shishlyannikov, S.M., Ravin, N.V., Mardanov, A.V., Beletsky, A.V., and Likhoshway, Y.V. 2013. The structure of microbial community and degradation of diatoms in the deep near-bottom layer of Lake Baikal. *PLoS One* **8**, e59977.

Zhang, H., Wang, K., Shen, L., Chen, H., Hou, F., Zhou, X., Zhang, D., and Zhu, X. 2018. Microbial community dynamics and assembly follows trajectories of an early spring diatom bloom in a semi-enclosed bay. *Appl. Environ. Microbiol.* **84**, e01000-18.

Znachor, P., Simek, K., and Nedoma, J. 2012. Bacterial colonization of the freshwater planktonic diatom *Fragilaria crotonensis*. *Aquat. Microb. Ecol.* **66**, 87–94.